

Calibrating TP-AGB stellar models and chemical yields through resolved stellar populations in the Small Magellanic Cloud

Giada Pastorelli¹, Paola Marigo¹, Léo Girardi^{1,2}
and the STARKEY project team

¹ Dipartimento di Fisica e Astronomia Galileo Galilei, Università di Padova,
Vicolo dell'Osservatorio 3, 35122 Padova, Italy –
email: giada.pastorelli@studenti.unipd.it

² Osservatorio Astronomico di Padova – INAF, Vicolo dell'Osservatorio 5,
35122 Padova, Italy

Abstract. Most of the physical processes driving the TP-AGB evolution are not yet fully understood and they need to be modelled with parameterised descriptions. We present the results of the on-going calibration of the TP-AGB phase based on a complete sample of AGB stars in the Small Magellanic Cloud (SAGE-SMC survey). We computed large grids of TP-AGB models with several combinations of third dredge-up and mass-loss prescriptions with the COLIBRI code. The SMC AGB population is modelled with the population synthesis code TRILEGAL according to the space-resolved star formation history derived with the deep photometry from the VISTA survey of the Magellanic Clouds. We put quantitative constraints on the efficiencies of the third dredge-up and mass loss by requiring the models to reproduce the star counts and the luminosity functions of the observed Oxygen-, Carbon-rich and extreme-AGB stars and we investigate the impact of the best-fitting prescriptions on the chemical yields.

Keywords. stars: AGB and post-AGB, stars: mass loss, galaxies: Magellanic Clouds

1. Modelling the AGB populations in the SMC

A reliable calibration of TP-AGB models requires: 1) a robust measurement of the Star Formation History (SFH) of the SMC 2) a complete sample of observed AGB stars accurately classified 3) detailed TP-AGB models to be included in the population synthesis code. [Rubele et al. \(2018\)](#) derived the SFH, the reddening and the distance of 168 subregions of the SMC, for a total area of 23.57 deg², using the deep photometry of the VISTA Survey of the Magellanic Clouds (VMC, [Cioni et al. 2011](#)). The main advantages of using VMC data are the lower extinction in the near-infrared passbands and the photometry reaching the oldest main-sequence turn-off points, ensuring a robust estimate of the ages. Our calibration is based on the AGB candidate list by [Srinivasan et al. \(2016\)](#) (SR16). The AGB population is classified into Carbon-rich (C-rich), Oxygen-rich (O-rich), anomalous (a-AGB) and extreme AGB (X-AGB), on the basis of photometric criteria ([Boyer et al. 2011](#)) and complemented with the available spectroscopic information ([Ruffle et al. 2015](#), [Boyer et al. 2015](#)). The TP-AGB models are computed with the COLIBRI code ([Marigo et al. 2013](#)) in which we adopt a scheme that considers two regimes of mass loss: (i) “pre-dust mass-loss” ($\dot{M}_{\text{pre-dust}}$) and (ii) “dust-driven mass-loss” (\dot{M}_{dust}). We test two formalisms for $\dot{M}_{\text{pre-dust}}$: the modified [Schróder & Cuntz \(2005\)](#) relation ([Rosenfield et al. 2016](#)), and the algorithm developed by [Cranmer & Saar \(2011\)](#) (CS11), in which $\dot{M}_{\text{pre-dust}}$ is driven by the pressure of Alfvén waves in the chromosphere.

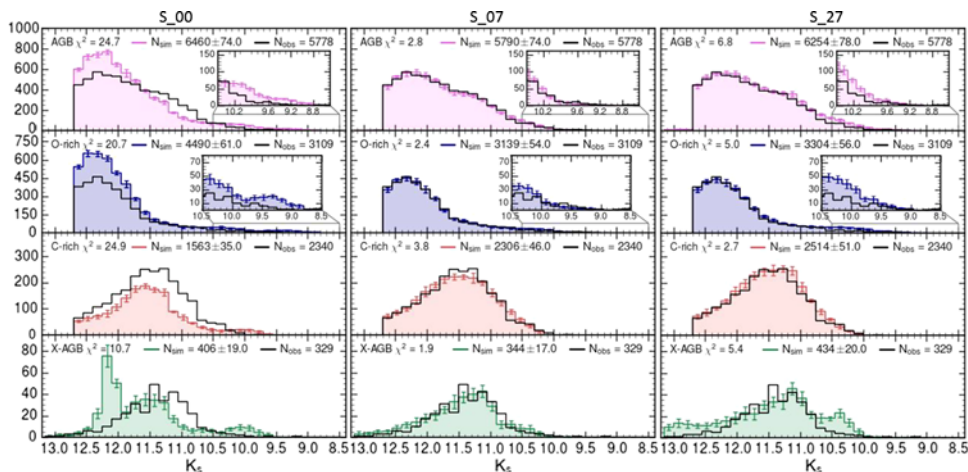


Figure 1. Mean K_s -band LFs of models S_00, S_07 and S_27 with error bars (coloured histograms), as compared to the observations (dark-line histogram) for the entire AGB sample and for the three main classes of AGB stars. The χ^2_{LF} specific to each panel is also reported.

During the dust-driven regime, we investigate a few among the most popular prescriptions of \dot{M}_{dust} , i.e. [Vassiliadis & Wood \(1993\)](#) and [Blöcker \(1995\)](#) (BL95). In addition, we use the recent results of dynamical atmosphere models by [Mattsson *et al.* \(2010\)](#) and [Eriksson *et al.* \(2014\)](#) (CDYN) for C-stars. The occurrence of a mixing event is checked with the T_p^{dred} parameter, i.e. the minimum temperature that should be reached at the base of the convective envelope at the stage of the maximum post-flash luminosity. The efficiency of each mixing event is described by the parameter λ , i.e. the fraction of the increment of the core mass during an inter-pulse period that is dredged-up at the next thermal pulse. For any combination of input prescriptions, we compute a complete set of TP-AGB tracks ($M_i = [0.5-6] M_\odot$; $Z_i = [0.0005-0.02]$), for a total of about 700 evolutionary tracks. Model quantities are converted into the relevant photometry as detailed in [Marigo *et al.* \(2017\)](#). We use the population synthesis code TRILEGAL ([Girardi *et al.* 2005](#)) to simulate each subregion covered by both VMC and SAGE-SMC surveys. Our primary calibrators are the star counts in the K_s -band Luminosity Functions (LFs) and K_s vs. $J-K_s$ CMD and we require the models to simultaneously reproduce these quantities for the O-, C-, and X-AGB star observed samples.

2. Calibration results

We start by simulating the SMC population using the TP-AGB tracks presented in [Marigo *et al.* \(2017\)](#) (S_00, left panel of Fig. 1). The total number of AGB stars is reproduced to within 10 per cent, in agreement with the previous calibration on low-metallicity dwarf galaxies ([Rosenfield *et al.* 2016](#)). However, there are evident discrepancies in the O-rich, C-rich and X-AGB LFs. First, we calculate a series of seven models exploring the effect of different mass-loss prescriptions for both O- and C-rich stars, while keeping the same prescriptions for the 3DU. We adopt the CS11 formalism for $\dot{M}_{pre-dust}$ and for the C-stars in the dust-driven regime we adopt the CDYN results. The sequence of models is computed by increasing the efficiency parameter of the B95 prescription applied to the M-stars, with η_{dust} ranging from 0.02 to 0.06. This results in a relatively modest effect on the total number of O-rich stars, whereas a significant impact shows up on the predicted C-rich LF. The reason is that the bulk of O-rich stars have low-mass progenitors and their lifetimes are mainly affected by the $\dot{M}_{pre-dust}$, whereas the B95 relation mainly

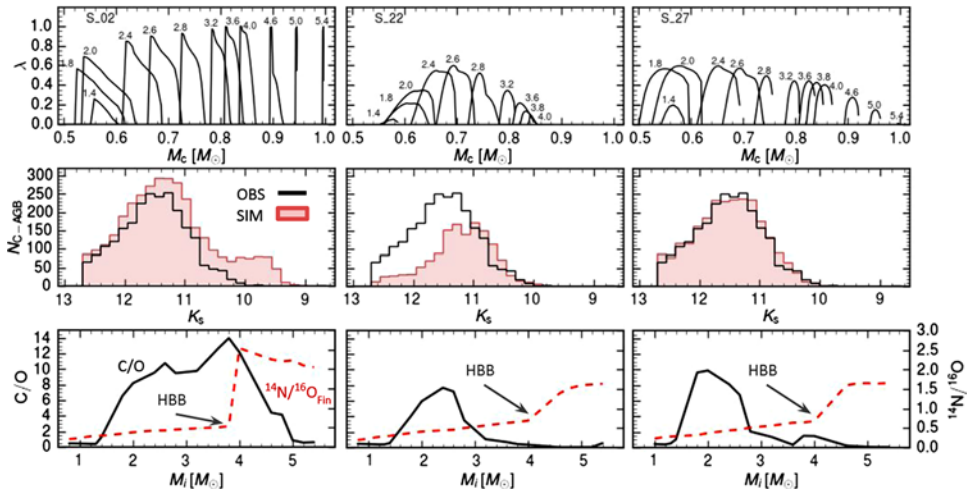


Figure 2. Top rows: efficiency of the 3DU (λ) as a function of the core mass M_c of a few selected evolutionary tracks with $Z_i=0.004$ and M_i as indicated. Middle rows: observed (black histograms) and simulated C-stars LFs as derived from the corresponding sets of models. The models share the same input prescriptions but for the onset and the efficiency of the 3DU. Bottom rows: final C/O and $^{14}\text{N}/^{16}\text{O}$ ratio.

affects the evolution of more massive (and brighter) AGB stars due to its high luminosity dependence. The best-fitting model of this first series (S.07, middle panel of Fig. 1) provides reasonably correct TP-AGB lifetimes, for the assumed 3DUP description, but the comparison with semi-empirical initial-to-final mass relations (IFMRs) (El-Badry *et al.* 2018; Cummings *et al.* 2018) reveals that such models tend to underestimate the White Dwarf (WD) masses for $M_i \gtrsim 3M_\odot$. We compute a second series of models with lower mass-loss efficiency ($\eta_{\text{BL95}} = 0.01 - 0.03$), focusing on the calibration of 3DU parameters and taking into account also the IFMR constraints. In Fig. 2 we show some of the fundamental steps that lead us to find a reasonable parametrisation of the 3DUP. We find that in order to reproduce the C-star LF (model S.27 in Fig. 2) and the LFs of O-rich, X-AGB, and the AGB sample, in addition to the final WDs masses, we need to keep a lower mass-loss efficiency and a lower efficiency of the 3DU for stars with $M_i \gtrsim 3M_\odot$ ($Z_i=0.004$). Different 3DU parametrisations have a large impact on the resulting chemical yields as shown in the lower panels of Fig. 2, which we are currently investigating.

Acknowledgements

We acknowledge the support from the ERC *project STARKEY*, G.A. n. 615604.

References

- Blöcker, T. 1995, *A&A*, 297, 727
 Boyer, M. L., McDonald, I., Srinivasan, S., Zijlstra, A., van Loon, J. T., Olsen, K. A. G., & Sonneborn, G. 2015, *ApJ*, 810, 116
 Boyer, M. L., Srinivasan, S., van Loon, J. T., McDonald, I., Meixner, M., Zaritsky, D., Gordon, K. D., Kemper, F., Babler, B., Block, M., Bracker, S., Engelbracht, C. W., Hora, J., Indebetouw, R., Meade, M., Misselt, K. 2011, *AJ*, 142, 103.
 Cioni, M.-R. L., Clementini, G., Girardi, L., Guandalini, R., Gullieuszik, M., Miszalski, B., Moretti, M.-I., Ripepi, V., Rubele, S., Bagheri, G., Bekki, K., Cross, N., de Blok, W. J. G., de Grijs, R., Emerson, J. P., Evans, C. J., Gibson, B., Gonzales-Solares, E., Groenewegen, M. A. T., Irwin, M., Ivanov, V. D., Lewis, J., Marconi, M., Marquette, J.-B., Mastropietro,

- C., Moore, B., Napiwotzki, R., Naylor, T., Oliveira, J. M., Read, M., Sutorius, E., van Loon, J. T., Wilkinson, M. I., & Wood, P. R. 2011, *A&A*, 527, A116
- Cranmer, S. R., & Saar, S. H. 2011, *ApJ*, 741, 54
- Cummings, J. D. and Kalirai, J. S. and Tremblay, P.-E. and Ramirez-Ruiz, E. & Choi, J. [arXiv:1809.01673](https://arxiv.org/abs/1809.01673)
- El-Badry, K., Rix, H.-W., & Weisz, D. R. 2018, *ApJ* (Letters), 860, L17.
- Eriksson, K., Nowotny, W., Höfner, S., Aringer, B., & Wachter, A. 2014, *A&A*, 566, A95.
- Girardi, L., Groenewegen, M. A. T., Hatziminaoglou, E., & da Costa, L. 2005, *A&A*, 436, 895
- Karakas, A. I., Lattanzio, J. C., & Pols, O. R. 2002, *PASA*, 19, 515
- Marigo, P., Bressan, A., Nanni, A., Girardi, L., & Pumo, M. L. 2013, *MNRAS*, 434, 488
- Marigo, P., Girardi, L., Bressan, A., Rosenfield, P., Aringer, B., Chen, Y., Dussin, M., Nanni, A., Pastorelli, G., Rodrigues, T. S., Trabucchi, M., Bladh, S., Dalcanton, J., Groenewegen, M. A. T., Montalbán, J., & Wood, P. R. 2017, *ApJ*, 835, 77
- Mattsson, L., Wahlin, R., & Höfner, S. 2010, *A&A*, 509, A14.
- Rosenfield, P., Marigo, P., Girardi, L., Dalcanton, J. J., Bressan, A., Gullieuszik, M., Weisz, D., Williams, B. F., Dolphin, A., & Aringer, B. 2014, *ApJ*, 790, 22.
- Rosenfield, P., Marigo, P., Girardi, L., Dalcanton, J. J., Bressan, A., Williams, B. F., & Dolphin, A. 2016, *ApJ*, 822, 73.
- Rubele, S., Pastorelli, G., Girardi, L., Cioni, M.-R. L., Zaggia, S., Marigo, P., Bekki, K., Bressan, A., Clementini, G., de Grijs, R., Emerson, J., Groenewegen, M. A. T., Ivanov, V. D., Muraveva, T., Nanni, A., Oliveira, J. M., Ripepi, V., Sun, N.-C., & van Loon, J. T. 2018, *MNRAS*, 478, 5017
- Ruffle, P. M. E., Kemper, F., Jones, O. C., Sloan, G. C., Kraemer, K. E., Woods, P. M., Boyer, M. L., Srinivasan, S., Antoniou, V., Lagadec, E., Matsuura, M., McDonald, I., Oliveira, J. M., Sargent, B. A., Sewilo, M., Szczerba, R., van Loon, J. T., Volk, K., & Zijlstra, A. A. 2015, *MNRAS*, 451, 3504
- Schröder, K.-P. & Cuntz, M. 2005, *ApJ* (Letters), 630, L73
- Srinivasan, S., Boyer, M. L., Kemper, F., Meixner, M., Sargent, B. A., & Riebel, D. 2016, *MNRAS*, 457, 2814
- Vassiliadis, E., & Wood, P. R. 1993, *ApJ*, 413, 641

Discussion

VENTURA: Which is the fraction of HBB stars within the X-AGB sample of the SMC? Do you believe possible a calibration of Hot Bottom Burning by the study of these bright sources

PASTORELLI: Our two best-fitting models predict a number of HBB stars around ten within the X-AGB sample. A calibration of the HBB using these sources would be possible if such stars could be clearly identified in the observations. In the K_s vs. $J-K_s$ CMD they are not always clearly distinguishable, but we can use other combinations of near- and mid-infrared colours to identify them and eventually perform a HBB calibration.

SRINIVASAN: Thanks for showing us the excellent agreement between your models and the observed K_s -band LF. Have you compared your prescription for circumstellar reddening with the Spitzer (e.g. 8 μm) LF? Do you find similar agreement?

PASTORELLI: Yes, we find a very good agreement with the Spitzer LFs and also with several combinations of colour-colour diagrams